Chemistry & Biology, Vol. 12, 769–777, July, 2005, ©2005 Elsevier Ltd All rights reserved. DOI 10.1016/j.chembiol.2005.05.012

Phosphoproteomic Analysis with a Solid-Phase Capture-Release-Tag Approach

Huang-Chun Tseng,[1,2,*] Huib Ovaa,[2,3] Nancy J.C. Wei,[2] Hidde Ploegh,[2] and Li-Huei Tsai[1,2,*]
[1]Howard Hughes Medical Institute
[2]Department of Pathology
Harvard Medical School
Boston, Massachusetts 02115

Summary

A comprehensive study of global phosphorylation events in biological systems is critical. We report a chemistry-based capture-release-tag method for isolation of complex phospho-Ser/Thr-containing peptides by liquid β-elimination combined with solid-phase Michael addition. The free thiol groups of 6-(mercapto-acetylamino)-hexanoic acid functionalized resin are used as immobilized Michael donors to capture dehydro-serine/threonine peptides. After an acid-mediated release step, phospho-peptides are labeled with a 6-(2-mercapto-acetylamine)-hexanoic amide tag at phosphorylated sites. We applied this method to analyze the phosphorylation status of microtubule-associated proteins. We find that a CDK5 substrate microtubule-associated protein 2 (MAP2) is phosphorylated on residues that are within a homologous region of Tau. The chemical method corroborates previous results and suggests that Tau and MAP2 may contain a CDK5 phosphorylation motif.

Introduction

In the postgenomic era, functional proteomics will accelerate the understanding of complicated biological pathways regulated by enzymatic activities [1]. Protein phosphorylation/dephosphorylation catalyzed by protein kinases/phosphatases is essential in a variety of signaling processes [2, 3]. However, methods for enriching phosphorylated epitopes from cells or tissues remain to be improved [4].

β-elimination of phosphates on serine and threonine residues under alkaline conditions is increasingly utilized for phosphorylation analysis [5–9]. The resulting dehydroalanine/dehydrobutyric acid subsequently serves as a Michael acceptor [5, 6]. Previous studies showed that sulfur nucleophiles are able to form covalent thioether bonds at phospho-serine/threonine residues during Michael addition [5, 10]. Recently, Oda et al. applied a liquid-phase β-elimination-based reaction followed by a NeutrAvidin bead purification to enrich phospho-peptides from yeast [6]. Surprisingly, only one phospho-peptide was obtained from this yeast phospho-proteome study [6], raising a concern of feasibility for using β-elimination/Michael addition for in vivo phospho-proteomic studies. In another study, Knight et al. designed a phosphorylation-specific proteolysis application using the elimination methodology to yield lysine-like residues at phosphorylation sites [7]. Whether this method is practical for complex cellular samples is still unclear. In this report, we took advantage of the ease of chemical diversification and the large reactive surface area of spherical matrix (resins), routinely used in solid-phase peptide syntheses, to design a novel approach that combines β-elimination chemistry with solid-phase Michael addition in a convenient one-pot procedure. Using a well-established kinase-substrate paradigm, we show that cyclin-dependent kinase 5-phosphorylated Tau protein can be captured and identified using solid-phase Michael addition from the whole-cell system and mouse brains.

*Correspondence: huang-chun_tseng@hms.harvard.edu (H.-C.T.); li-huei_tsai@hms.harvard.edu (L.-H.T.)
[3]Present address: Netherlands Cancer Institute, Division of Cellular Biochemistry, 1066 CX Amsterdam, the Netherlands.

Results and Discussion

Our approach, termed solid-phase Michael addition (SMA), for isolation of β-elimination-sensitive phospho-peptides is illustrated in Figure 1A. Briefly, cysteine residues of tryptic phospho-peptides are reduced and alkylated. The core chemical reactions, β-elimination and solid-phase Michael addition, occur under alkaline reaction conditions. Phospho-serine and -threonine are converted to dehydroalanine and dehydrobutyric acid, respectively. Newly formed double bonds between the α and β carbons of dehydroalanine/dehydrobutyric acid subsequently serve as Michael acceptors to which nucleophilic resins react. In contrast to previously reported liquid-phase Michael addition-based methods [6–9, 11], phospho-peptides are directly captured by the solid Michael-addition resins. Unreacted peptides and debris are washed away while phospho-peptides form a covalent linkage and remain on the resin. Captured peptides in tagged form are released by trifluoroacetic acid-mediated cleavage of the amine bond. The chemical structure of the nucleophilic group used in the resin is depicted in Figure 1B. The molecular mass of the tag moiety is 203.09 Daltons (Figure 1B) and the delta mass at serine/threonine residues is 186.12 Daltons. The negatively charged phosphate is substituted with an amide-containing tag after SMA treatment. Phosphorylation sites on released products are subsequently determined by liquid chromatography-coupled tandem mass spectrometry.

To determine whether our resin can capture phosphate-containing peptides, a phospho-Ser peptide derived from the cyclic-AMP responding element binding (CREB) protein was tested in the early stage of method development. After SMA treatment, the chemically tagged products were analyzed by matrix-assisted laser desorption/absorption ionization-time of flight mass spectrometry (MALDI-TOF MS). We found that the major molecular ions at mass/charge (m/z) 1796.97, representing the phosphorylated form of the CREB peptide (Figure 1C1), shifted to a higher m/z value of 1903.02 (Figure 1C2). This value matched the theoretical m/z

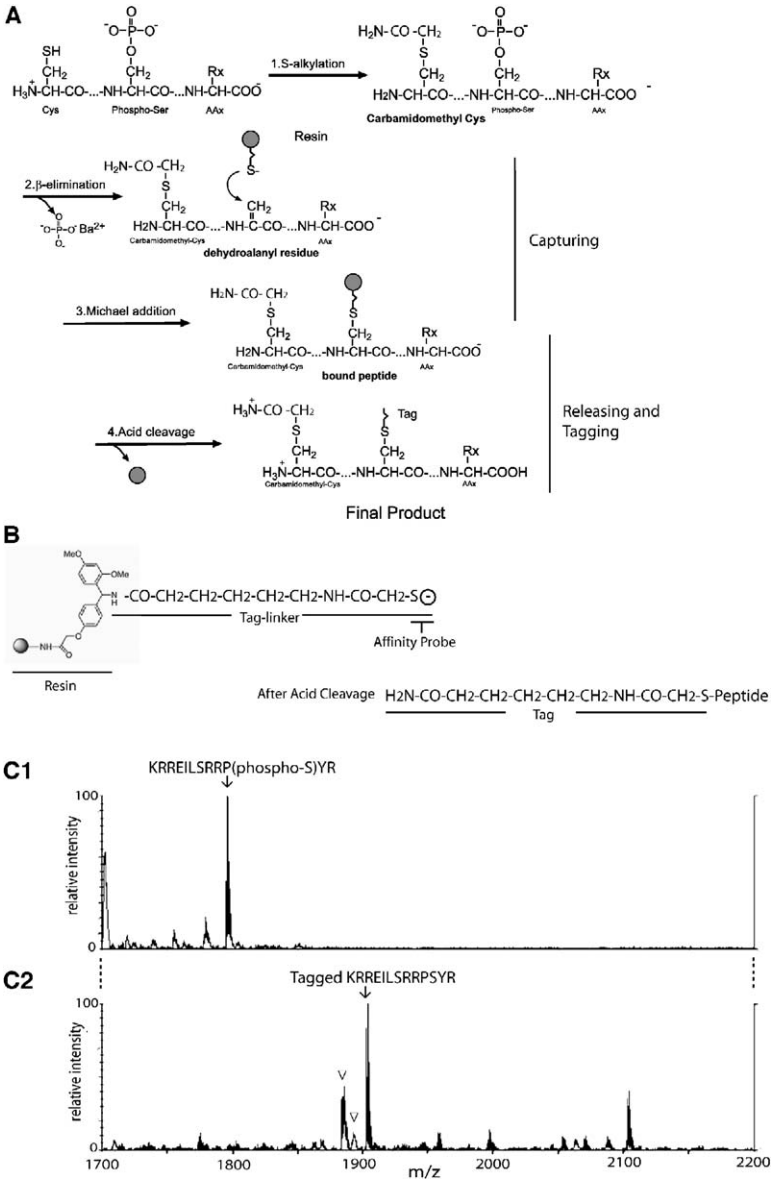

Figure 1. Scheme and Proof-of-Principle of Solid-Phase Michael Addition Metholodogy

(A) The method involves a sample preparation step (1. alkylation), a capturing step (2. β-elimination and 3. Michael addition), a washing step (between 3 and 4), and a tag-releasing step (4. acid-mediated cleavage).

(B) Detailed chemical structure of 6-(2-mercapto-acetylamine)-hexanoic acid RINK resin.

(C) MALDI-TOF mass spectra of 1 pmol phospho-CREB peptides (1) before SMA treatment and (2) after SMA treatment. Metastable ions are indicated by arrowheads.

value of the tagged-CREB peptide, suggesting that the phosphate-containing CREB peptide was captured by the resin and the phosphate group of the peptide was replaced with the tag moiety. A side product at m/z 2103.05 was also detected (Figure 1C2). Potential side reactions in SMA are discussed below. Similar CREB peptide capture results were observed on four different resin preparations. To investigate the specificity of SMA, we attempted to isolate the phospho-CREB peptide (1 pmol) from a nonphosphoryl peptide library with KSYGXEXTLXAE sequences (X = any amino acids except cysteine, 6859 different peptides in total, approximate weight ratio of the peptide library to the CREB peptide = 8000:1). The results showed that SMA was able to specifically capture and tag the phospho-CREB peptide as judged by MALDI-TOF analysis (see Figure S1 in the Supplemental Data available with this article online). SMA did not isolate nonphosphoryl peptides (Figure S1C). In addition to phospho-Ser-containing peptides, we found that SMA was able to capture and tag a synthetic phospho-Thr peptide with a VDAAV(pT)-PEERH(carbamidomethyl-C) sequence (data not shown).

In addition to assessing the specificity of SMA, the yield of capturing phospho-peptides was also evaluated. One nmol of CREB phospho-peptide was incubated with 50 μl of resin (provides approximately 10 μmol of functionalized ligand). Upon treatment with SMA, all of the input peptide (1 nmol) was efficiently recovered (Figure S1). No phospho- and dehydro-form of the CREB peptides were detected in the unbound fraction (Figure S1F). To test for sensitivity, 50 μl of the SMA resin was incubated with various amounts of phospho-CREB peptide. The resin was able to recover synthetic phospho-peptides from concentrations as low as 250 fmol of pure CREB phospho-peptide as judged by MALDI-TOF measurement (data not shown).

Together, these results suggest that the thio-nucleophilic resin can specifically capture, release, and tag phospho-serine/threonine-containing peptides.

To demonstrate the SMA chemistry and its application for acquiring biological information from complex samples, we focused on the CDK5-mediated phosphorylation of microtubule-associated proteins. The longest isoform of the human microtubule-associated protein Tau is composed of 441 amino acid residues, among which 45 residues are serine and 35 are threonine [12]. Phosphorylation events regulate the interaction between Tau and microtubules [13] and facilitate the formation of neurofibrillary tangles in Alzheimer's disease (AD) [14, 15]. At least 29 sites on AD-Tau are phosphorylated by a variety of serine/threonine kinases including PKA, GSK3β, and CDK5 [16–18]. Currently, research on Tau phosphorylation is restricted to a limited number of phosphorylation-specific antibodies, which cannot reveal the heterogeneous phosphorylation status of Tau. Therefore, analysis of global Tau phosphorylation states by improved proteomic methods is desirable as it can contribute to a better understanding of the mechanism underlying AD.

CDK5 is a proline-directed protein kinase essential for development of the mammalian central nervous system [19]. CDK5 requires association with a regulatory activator p35 to become active. Calpain-dependent cleavage of p35 to p25 has been implicated in the pathogenesis of AD [20]. While CDK5/p35 is a poor Tau kinase, CDK5/p25 has been shown to cause hyperphosphorylation of Tau [20, 21]. 100 pmol of recombinant Tau protein was phosphorylated in vitro by purified CDK5/p25 to a stoichiometry of 0.5 phosphates per Tau molecule. Tryptic peptides derived from the unphosphorylated or phosphorylated Tau protein were first analyzed by MALDI-TOF MS (Figures 2A and 2B). One peak at m/z = 1473.60 matched the mass of a monophospho-peptide SGYSSPGSPGTPGSR in samples phosphorylated by CDK5 (Figure 2B). This monophospho-peptide did not appear in the control sample without kinase incubation (Figure 2A). The signal intensity of the phospho-peptide diminished after phosphatase treatment (Figure 2C). The tryptic peptide samples containing phosphorylated and dephosphorylated peptides were further analyzed by SMA. One molecular ion corresponding to the mass of SGYSSPGSPGTPGSR plus one tag (m/z 1579.72) was observed in the phosphorylated sample (Figure 2D) but not in the dephosphorylated sample (Figure 2E). A previous report showed that minor β-elimination may occur at serine/threonine residues in the absence of phosphates [8]. However, we did not observe such side reactions (Figure 2E). These data suggest that SMA isolated the phosphorylated form of the peptide, but not the unphosphorylated form. In addition to isolating peptides, SMA was also tested for isolation of phospho-Tau proteins. However, the method failed to isolate full-length phospho-Tau prior to trypsin digestion, suggesting that the solid-phase procedure is more efficient in capturing phospho-peptides than full-length proteins.

IMAC is another method for enriching phospho-peptides [22]. To compare IMAC and SMA, we used an iron (III)-nitriloacetic acid gel (an IMAC) to enrich for the Tau tryptic peptide pool shown in Figure 2B. A MALDI-TOF spectrum of IMAC-isolated peptides showed that IMAC was able to isolate the same SGYSSPGSPGTPGSR phospho-peptide isolated by SMA (Figure 2F). These results suggest that both SMA and IMAC can enrich for phosphorylated peptides. However, three acidic residue-rich nonphospho-peptides QEFEVMEDHAGTYGLGDR (m/z 2053.89), DQGGYTMHQDQEGDTDAGLK (m/z 2165.90), and KDQGGYTMHQDQEGDTDAGLK (m/z 2293.99) were also enriched by the IMAC approach (Figure 2F). This may be due to the preferential enrichment of acidic peptides by IMAC [4]. The overall complexity of recovered peptides by SMA is less than that obtained by IMAC. Thus, one advantage of SMA over IMAC is that it yields less background unphosphorylated peptides after enrichment, increasing the probability of detecting low-abundance phosphorylation events.

We further used tandem mass spectrometry to analyze the SMA-treated Tau peptides in order to gain sequence information from fragmented peptide ions. A collision-induced dissociation spectrum obtained from an ion-trap instrument showed a parent ion of m/z 790.35 (2+) containing the SGYSSPG (tag-S)PGTPGSR peptide (Figure S2B). The same molecular ion was also detected and analyzed in a quadrupole-time of flight instrument. A quadrupole-time of flight ms/ms spectrum was acquired (data not shown) and the same peptide sequence was detected as that detected from the ion-trap MS spectrum. The theoretical immonium ion of the tagged serine residue is not observed at the low mass range, suggesting that the precursor ion scan type of measurement may not be useful to detect phospho-peptides isolated by SMA treatment. Three major daughter ions, *y*4, *y*7, and *y*10, were detected in the spectrum (Figure S2B), indicating the presence of proline-induced fragmentation [23]. Background peaks or side products shown in Figures 2D and 2E did not provide valid peptide sequence information in tandem mass spectrometry analysis. Fragmentation of those background peaks in MS/MS analysis did not display a classic peptide fragmentation pattern and was not interpreted by the MASCOT algorithm to a confident level. The SGYSSPG (tag-S)PGTPGSR is the only valid result, suggesting that the side products do not adversely affect phosphorylation determination.

To further verify the sites on Tau phosphorylated by CDK5, we used available phospho-Tau antibodies to probe in vitro phosphorylated Tau. AT-8 antibody, raised against phospho-S202/T205 of Tau [24], recognized in vitro CDK5-phosphorylated Tau (Figure S2A). Conversely, T231 of Tau is not an ideal substrate for CDK5 [18], and neither SMA nor the phosphorylation-specific antibody pT231 (Figure S2A) detected the phosphorylation of this residue by CDK5. Thus, these phospho-epitope-specific antibodies confirm the SMA-determined phosphorylation status of Tau.

To study Tau phosphorylation in a more biologically relevant context, we transfected human Tau with or without the active CDK5 complex in neuroblastoma CAD cells. Heat-stable protein samples (250 μg) prepared from transfected cells were treated with SMA followed by tandem mass spectrometric analysis. Results showed that residues T169, T181, S185, S191, S195, S198, S199, S202, T205, S208, S210, T217, T220, S241,

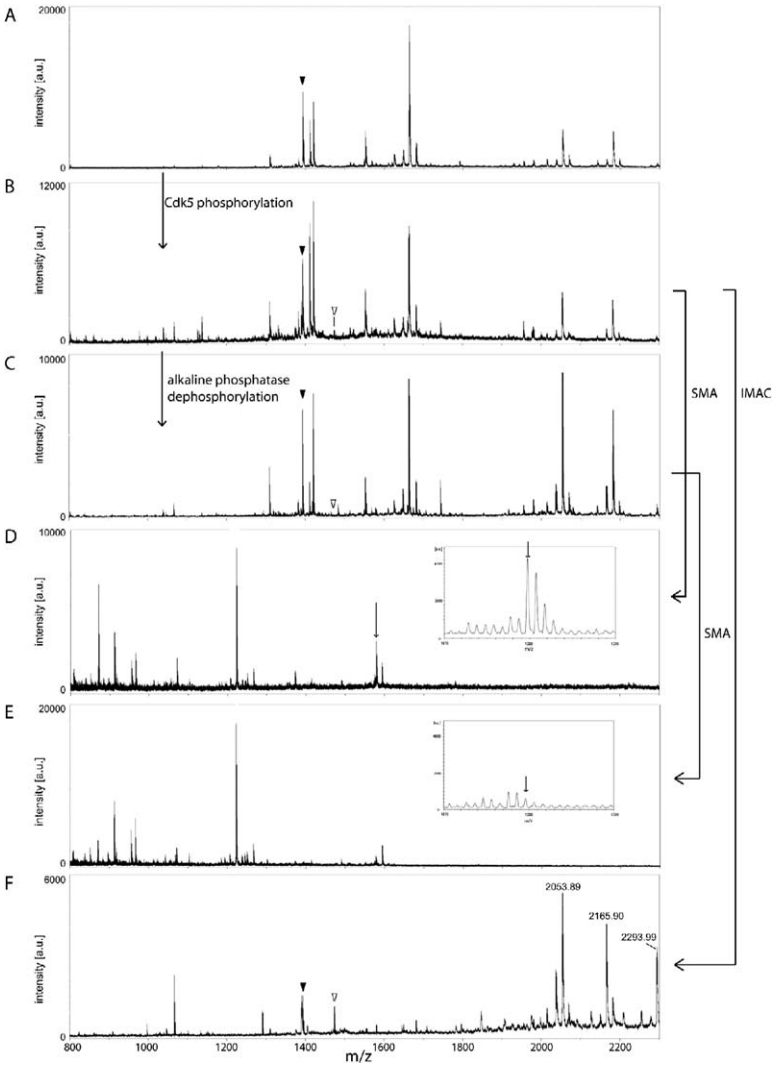

Figure 2. MALDI-TOF Mass Spectrometric Analysis of Phosphorylated Tau

Recombinant Tau (100 pmol) was phosphorylated by active CDK5 in vitro. Tryptic Tau peptides prepared from samples in the absence and presence of active CDK5 are shown in (A) and (B), respectively. As a control, CDK5-phosphorylated peptides were treated with alkaline phosphatases. The MS spectrum of dephosphorylated peptides is shown in (C). After a peptide mass fingerprint analysis, one phospho-peptide, SGY SSPGSPGTPGSR, plus 1 phosphate was detected and is indicated by an arrow. The non-phospho-peptide counterpart is indicated by an arrowhead. The phosphorylated and dephosphorylated samples were prepared by SMA prior to MS analysis ([D] and [E], respectively). The peptide with the tag, representing the phospho-peptide, is detected in spectrum (D), but not in (E). The phospho-peptide was also isolated by using IMAC, another technique for enriching phospho-peptides (F).

S396, and T403 were phosphorylated (Figure 3B, Table S1). Among these residues, T181, S199, S202, T205, T217, and S396 are (S/T)P sites representing the CDK5-phosphorylation motif and were previously reported CDK5 sites [18, 25–29]. Immunoblots using phospho-Tau antibodies showed that phosphorylation of S202, T205, and S396 was significantly increased, whereas no phosphorylation of T231 was detected in the sample prepared from CDK5/p25/Tau triple transfected CAD cells (Figure 3A), supporting results obtained by SMA followed by mass spectrometry (Table S1). Most phospho-Tau peptides listed in Table S1 were not detected in the PKA-Tau-transfected controls (phosphorylation control) or in an unfunctionalized resin control (nonspecific binding control) (data not shown). We previously reported the phosphorylation of endogenous Tau in the brain of a p25-overexpressing mouse model using conventional tandem mass spectrometry [30]. Here, we found extensive overlap of phosphorylation sites detected in the animal model and the cell-based system, including S195, S198, S199, S202, T205, S217, T220, S396, and T403. Phosphorylation at S185, S191, S208, and S210 discovered in this report are novel phosphorylation sites.

The detection of non-(S/T)P phosphorylation sites (T169, S185, S191, S195, S198, S208, S210, T220, S241, and S403 in Figure 3B) that do not correspond to the CDK5 phosphorylation motif suggests that overexpressed Tau in CAD cells is also phosphorylated by other Ser/Thr kinases. Some peptides were multiply tagged (Table S1), suggesting that the resin can label multiple phosphorylation sites on the same peptide. The presence of disulfide-linked tag dimers after the acid cleavage suggests that the spatial proximity of adjacent ligands allows the reactions of multiple tags on one peptide to occur. We note that not all phosphates were replaced by the chemical tag. That may be due to the alkaline strength of SMA β-elimination condition. Another speculation suggests that β-elimination is influenced by the sequence, composition, and structure of peptides. Nevertheless, both the tagged and phosphorylated forms of serine and threonine can be simultaneously identified by tandem mass spectrometry.

In addition to phospho-Tau peptides, we also de-

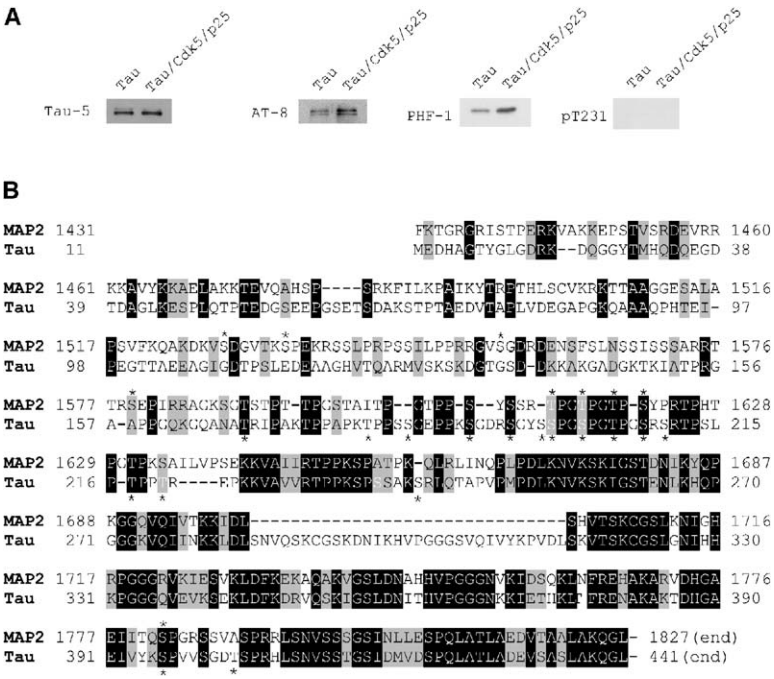

Figure 3. Detection of Tau and MAP2 Phosphorylation in a Whole-Cell System

(A) Immunoblotting assay of Tau proteins. Tau-5 is an antibody recognizing total Tau. AT-8 antibody recognizes phosphorylation of S202/T205 of Tau. PHF-1 specifically recognizes phospho-S396. pThr231 antibody recognizes phosphorylation of T213 at Tau.

(B) Comparison of CDK5-mediated phosphorylation of MAP2 and Tau in CAD cells. Partial sequences of MAP2 (NCBI access number NP_002365) and Tau (access number QRHUT1) are shown. Pairwise alignment of MAP2 and Tau was done with the BioEdit software using the PAM120 algorithm. Black blocks indicate identical amino acids; gray blocks indicate amino acids with similar chemical and physical properties. Dashes represent probable gaps. Phosphorylation sites detected in CDK5-active cells were labeled with stars. Note that most of the similar phosphorylation sites of the two proteins appear in the highly homologous regions.

tected phospho-peptides derived from other cellular proteins in CAD cells. Among these proteins, we discovered a phosphopeptide corresponding to microtubule-associated protein 2 (MAP2), a potentially novel CDK5 substrate. We decided to focus on MAP2 because it shares nearly identical microtubule binding repeats and a proline-rich region [31] with Tau. Like Tau, MAP2 is also phosphorylated by multiple kinases [32]. However, information on the specific phosphorylation sites are limited and it is not known whether CDK5 phosphorylates MAP2 in cells [32]. Using SMA, we found that endogenous MAP2 was phosphorylated in cells transfected with Tau alone (Table S1). This supports a previous study that MAP2 is constitutively phosphorylated in vivo [33]. In the control sample, phosphorylation at residues T1452, T1507, S1514, S1519, S1528, and S1555 was detected (Table S1). In CDK5-active cells, residues S1528, S1534, S1555, T1613, T1616, T1619, S1621, and S1782 were phosphorylated (Table S1). Interestingly, in CDK5/p25-expressing cells, specific phosphorylation of MAP2 was limited to (S/T)P sites (S1534, T1613, T1616, T1619, and S1782 in Table S1), whereas phosphorylation events at S1528 and S1555 appeared in both control and CDK5-activated cells. Among these (S/T)P phosphorylation sites, T1613/T1616/T1619 and S1782 on MAP2 are at analogous regions of S199/S202/T205 and S396 on Tau, the two main CDK5 phosphorylation modules of Tau (Figure 3B). The sequence 1613TPGTPGTP1620 is located in the proline-rich region of MAP2, and phosphorylation of this proline-rich region was observed in growth regions of rat hippocampal neurons [34]. In an in vitro phosphorylation experiment, purified CDK5/p25 was able to phosphorylate (S/T)PG(S/T)PGTP peptides and purified MAP2 (data not shown). Thus, with the use of SMA, we were able to identify a novel CDK5 substrate that was further confirmed by in vitro phosphorylation.

Previous studies showed that CDK5 preferably phosphorylates the (S/T)PX(K/H/R) sequences [35]. Our results suggest that 1613TPGTPGTP1620 of MAP2 and 199SPGSPGTP206 of Tau may represent another CDK5 phosphorylation motif, (S/T)PG(S/T)PGTP. Furthermore, this motif features two consecutive PXXP sequences known to be SH3 domain binding sites [36, 37]. Phosphorylation of this motif influences binding of the SH3 domain of the protein tyrosine kinase Fyn to Tau [38] and binding of the prolyl isomerase Pin1 to Tau [39]. The binding of Src to MAP2 is inhibited by phosphorylation of MAP2 by MAPK and ERK2, but not by PKA [37]. It is tempting to speculate that CDK5 phosphorylation of this motif on MAP2 may have similar effects as that observed on Tau. However, additional evidence for direct regulation of MAP2 by CDK5 is necessary to test this hypothesis.

To understand the basal phosphorylation status of the heat-stable proteins in vivo, we treated 250 μg of tryptic peptides derived from the heat-stable fraction of mouse forebrains with SMA. We detected a total of 205 peptides from 999 MS/MS spectra. Among those peptides, there are 105 phospho-peptides and 184 phosphorylation sites (Table S2). The majority of recovered phospho-peptides were mono-phospho-peptides (41%) and di-phospho-peptides (46%). Tri-phospho-peptides and quadru-phospho-peptides encompass only 12% of the total phospho-peptides. One peptide derived from Tau, 526SPSASKSR533 (numbering based on 732 amino acid-long Tau) was tagged at residues S526 and S532 (or S235 and S241 on 441 amino acid-long Tau in Figure 3). The phosphorylation sites on the MAP2 peptide, 1650TPPKSPATPK1659 (Table S2), correspond to phosphorylation of T1649, S1653, and T1656 in human MAP2 (Figure 3).

In summary, a plethora of techniques have been developed to aid in mass spectrometry-based phospho-

proteomic analysis, including phospho-specific antibodies, affinity chromatography, chemical modification, precursor ion scanning, neutral-loss scanning, and electron capture dissociation techniques [4, 7, 40]. The feasibility of β-elimination/Michael addition for phospho-peptide analysis was raised by a previous report [6]. Here we present evidence that our novel solid-phase procedure is able to efficiently isolate and identify phospho-peptides from whole-cell systems. There are several notable discrepancies between our and previously published procedures. First, the labeling of phosphorylation sites and enrichment of phospho-peptides by our method occurs in a single solid-phase one-pot reaction, which may reduce the likelihood of sample loss. This one-pot reaction is different from previous attempts that perform β-elimination and Michael addition in the liquid phase, followed by a separate solid-phase extraction to recover peptides [6, 8, 9] Second, the mass of the 6-(2-mercapto-acetylamine)-hexanoic amide tag, which is smaller than a previously described biotin tag [6], allows for a wider detection window in the mass spectrometric measurement. Third, a previous study reports that replacement of a phosphate with an amine-containing moiety at phosphorylation sites can enhance phospho-peptide detection in mass spectrometry [7]. We failed to detect neutral-loss of the 6-(2-mercapto-acetylamine)-hexanoic amide tag by MALDI-TOF MS analysis (Figures 1C2 and 2D) or by tandem mass spectrometric analysis (data not shown), suggesting that the tag is a more stable moiety than a phosphate. Fourth, we use barium hydroxide, which is more efficient than sodium hydroxide or potassium hydroxide reported previously, to catalyze β-elimination [8, 41]. β-elimination may also occur on carbamidomethylated cysteinyl or *O*-linked glycosylated peptides [41]. In our hands, carbamidomethyl cysteinyl residues remain intact and do not undergo β-elimination. The use of barium hydroxide can significantly reduce the reaction rate of β-elimination of *O*-linked glycosylated peptides by two orders of magnitude compared to that of phospho-Ser/Thr peptides [41]. Thus, these potential side reactions should be very minor during SMA. Fifth, a minor side product 200.05 Daltons heavier than the tagged peptide is observed and forms an ion pair with the tagged peptide (Figure 1C2). We tested for occurrences of various potential side reactions, including iodination on tyrosine residue, oxidation on the sulfur of the SMA ligand and cysteine residues, dehydration of unphosphorylated serine/threonine residues, and unexpected acid cleavage sites on the RINK resin. However, none of these possibilities accounted for the minor side reaction observed during the SMA reaction. The side product cannot be explained by an additional tag added to unphosphorylated serine/threonine residues because the delta mass of an additional tag is 186.12 Daltons. Nevertheless, this side reaction does not have any adverse effects on data analysis. Dephosphorylation of phospho-peptides with phosphatases prior to SMA may serve as an additional control to ensure accurate phosphorylation determination.

Recently, Collins et al. showed that different IMAC protocols yield different coverage in phosphorylation site determination [42]. Our preliminary phospho-proteomic studies on mouse brains suggest that phospho-peptides recovered by SMA and IMAC are not entirely identical (unpublished result). It is likely that different methods of capturing phospho-peptides enrich different groups of phospho-peptides. A study of phosphorylation events on synaptic proteins showed that 351 phospho-peptides were recovered from approximately 18 mg of sample by IMAC approaches [42]. Classic IMAC and improved IMAC [40] likely isolate peptides with multiple phosphorylation sites [42]. The application of strong cation exchange chromatography combined with neutral-loss detection of phosphoric acid allowed detection of more than 2,000 phosphorylation sites among 525,000 MS/MS spectra when 8 mg of starting materials was used [43]. This strong cation exchange method prefers the isolation of monophospho-peptides [42]. In contrast, SMA is designed to target β-elimination-sensitive phosphorylation sites. The covalent bond linkage of the phospho-peptide to SMA resins is more stable during the non-phospho-peptide removal step than the ionic linkage in IMAC or strong cation exchange. SMA is expected to recover a wide range and yield a higher percentage of phospho-peptides. The phospho-proteomic analysis of mouse brain heat-stable proteins (Table S2) supports this notion. Additional analyses using whole cell or tissue samples are necessary to further examine the efficiency of SMA.

Significance

We present the first evidence for successful application of solid-phase Michael addition for the purpose of phospho-peptide enrichment. This report not only demonstrates mass spectrometry-based phosphorylation determination, but also extends the application of solid-phase chemistry to tag biological samples with phosphorylation modifications. The newly designed thio-nucleophilic resin fulfills two functions, the capturing and tagging of phospho-peptides in one single reaction vessel when β-elimination and Michael reaction occur. Solid-phase chemistry is conventionally applied to small molecule synthesis, chemical capturing, peptide synthesis, and reaction catalysis. This SMA application extends the solid-phase chemistry to labeling purposes. Furthermore, the novel SMA method will improve current detection of Ser/Thr phosphorylation reactions and broaden the understandings of biological processes and diseases.

Experimental Procedures

Materials

RINK resin (ArgoGel-RINK-NH-Fmoc) was purchased from Argonaut Technologies (San Carlos, CA). PyBOP (benzotriazole-1-yl-oxy-tris-pyrrolidino-phosphonium hexafluorophosphate) and SAMA-OPfp (S-acetylthioglycolic acid pentafluorophenyl ester) were purchased from Calbiochem-Novabiochem AG (Laufelfingen, Switzerland). Synthetic phospho-Ser CREB peptide was obtained from New England Biolabs. Phospho-Thr VDAAV(phospho-T)TEERHC peptide was synthesized at Tufts Core Facility, Tufts University (Medford, MA). Phos-Select iron affinity gel, an iron(III)-nitriloacetic acid gel, and MAP2 protein were obtained from Sigma-Aldrich (St. Louis, MO). Tau-5 (monoclonal) and Tau [pThr231] (polyclonal) antibodies were purchased from Biosource (Camarillo, CA); AT-8 (monoclonal) from Innogentics (Belgium). PHF-1 (monoclonal) antibody is a gift from M.D. Nguyen (Harvard Medical School). Horseradish peroxi-

dase (HRP)-conjugated AntiMouse/AntiRabbit IgG secondary antibodies were purchased from Amersham Biosciences (Piscataway, NJ). Chemiluminescence reagents used in immunoblotting assay were purchased from NEN Life Science Products (Boston, MA). All other compounds are reagent grade. The DNA constructs hTau40, CDK5-HA, and p25-HA were described previously [21]. Active CDK5/p25 complex was provided by Andrea Musacchio at European Institute of Oncology (Italy).

Synthesis of Nucleophilic RINK Resin

Synthesis of the resin is based on Fmoc chemistry to add the 6-(mercapto-acetylamino)-hexanoic acid group onto ArgoGel RINK-NH-Fmoc resin (approximate ligand stoichiometry, 0.3 mmol/gram of resin). Solid-phase peptide synthesis was carried out on an 180° Variable Rate Shaker (Peptides International, Louisville, KY). 2.5 grams (dry weight) of ArgoGel RINK-NH-Fmoc resin were first swelled in 20 ml of DMF solvent for 10 min at room temperature and then incubated in 50 ml of 20% piperidine/DMF solution for 1 hr at room temperature in order to remove the Fmoc group. After Fmoc removal, resins were washed extensively in DMF (*N*, *N*-dimethylformamide, American Bioanalytical, Natick, MA). Fmoc-ε-Ahx-OH (*N*-fluorenyl oxycarbonyl hexanoic acid, 5 equivalents to the number of RINK-NH-Fmoc moles on the resins) was preactivated with PyBOP (6 equivalents to the number of Fmoc-ε-Ahx-OH moles) and DIPEA (di-isopropylethylamine, 6 equivalents to the number of Fmoc-ε-Ahx-OH moles) in DMF for 2 min and added to the resin. After 30 min, the resin was washed extensively and followed by a second coupling overnight. A standard Fmoc removal procedure of the protective group was applied to remove the terminal Fmoc group. SAMA-OPfp (5 equivalents to the number of RINK-NH-Fmoc moles) was added in DMF and the resin was incubated for 30 min followed by a second coupling overnight. The terminal acetyl group on the ligand, which prevents the thiol group from oxidation during storage, was removed before use of the resin in DMF containing 10% ammonium hydroxide for 1 hr followed by extensive washing with DMF (3 times), ethanol (3 times), and water (3 times). Completion of each coupling step was monitored by the Kaiser test that detected free terminal amino groups in solid-phase synthesis of peptides [44]. Because of the absence of free amino groups after each synthesis step, all RINK-NH-Fmoc ligand are converted. An LCT LC-MS instrument (Waters, Milford, MA) was used to monitor the synthesis of the resin by analyzing acid-cleaved products.

β-Elimination and Solid-Phase Michael Addition

One-pot β-elimination and Michael addition reactions were effected in 10% acetonitrile and 20 mM $Ba(OH)_2$ (pH 10.5) in closed microcentrifuge tubes at 37°C under gentle agitation for 16 hr. Freshly prepared 2-mercaptoacetyl-hexanoyl functionalized beads (30 μl of bed volume) were used in a reaction with 1 pmol of synthetic polypeptides or with 500 μg of cellular polypeptides. Unfunctionalized RINK resin was used in parallel as a control to examine nonspecific binding. Reactions were terminated by adjusting the pH to 5 with acetic acid. Reaction solutions were removed and the resins were collected after brief centrifugation. Resins were subsequently washed in sequence with PBS (phosphate-buffered saline), 50% methanol, 90% acetonitrile, 100% DMF, and 100% methanol, with two washes in each solvent for 5 min. Resins were dried in a SpeedVac. Peptide cleavage was carried out by two steps of incubating 200 μl of 20% TFA (trifluoroacetic acid in water) to the resins at room temperature for 30 min each. A total of 400 μl of cleavage products was collected and the volume was reduced to 100 μl in a SpeedVac. Peptides in the TFA solution were precipitated in 1 ml of cold diethyl ether and collected after centrifugation at 15,000 × g for 10 min. The isolated peptides were dried in a SpeedVac and used for mass spectrometric analysis.

Cell Culture and DNA Transfection

Human neuroblastoma CAD cells were cultured in DMEM containing 10% fetal bovine serum, 2 mM L-glutamine, 100 units/ml penicillin, and 100 μg/ml streptomycin at 5% CO_2, 37°C. At 80%–90% confluence, cells were transferred to Opti-MEM media containing glutamine for transfections. Transfections were performed with Lipofectamine 2000 following the vender's protocol (Invitrogen, Carlsbad, CA). 20 μg of Tau contruct, 20 μg of CDK5 construct, and 20 μg of p25 construct were used for transfection of cells in one 150 cm^2 flask. 24 hr posttransfection, Opti-MEM medium was removed and cells were washed with cold PBS. To generate protein kinase A-Tau, CAD cells were transfected with Tau constructs for 24 hr followed by a 1 hr treatment with 10 μM foskolin (Sigma-Aldrich).

Preparation of Heat-Stable Protein Samples and Immunoblotting Assay

Transfected cells (2–4 × 10^7 cells) or mouse forebrain tissues (0.1–0.25 g) were homogenized and lysed in cold RIPA buffer (150 mM NaCl, 1% NP-40, 1 mM EDTA, 0.5% sodium deoxycholate, 0.1% SDS, 50 mM Tris [pH 8.0]) containing 1 mM DTT, 1 mM NaF, 1 mM Na_3VO_4, 10 nM calyculin-A, 100 nM cyclosporine A. Cell lysates were collected after short centrifugation to remove cell debris. Tau and MAP2 are heat-stable proteins that can be enriched by heat treatment [15]. Cell lysates were heated at 90°C for 5 min. Heat-stable protein lysates were collected by a 15,000 × g centrifugation for 10 min at 4°C. For immunoblotting, 1 μg of each protein sample was resolved on a 12% SDS-PAGE gel. Proteins were electro-transferred onto PVDF membranes. Tau-5 (1:500 dilution), AT-8 (1:1000), PHF-1 (1:500), and Tau[pS396] (0.5 μg/ml) were used for the primary antibody binding reaction. HRP-conjugated anti-mouse antibody (1:5000) or HRP-conjugated anti-rabbit antibody (1:5000) was used in secondary antibody binding. The labeled Tau proteins were visualized by chemiluminescence and film exposure.

Preparation of Peptides and IMAC Sample

Phospho-Thr VDAAV(phospho-T)PEERHC peptides (1 mg/ml) were incubated with iodoacetamide (10 mg/ml) for 30 min at room temperature in dark. The carbamodimethylation was quenched by addition of 8 mM DTT. Recombinant Tau was prepared as described previously [13]. The in vitro phosphorylation conditions of Tau (1 μg) was previously described [13], except that 50 ng of purified CDK5/p25 was used instead. The in vitro phosphorylation of MAP2 used the same condition as that of Tau. Phosphorylated Tau was digested with trypsin at a ratio of 100:1 (w/w) at 37°C overnight. Phosphorylation was stopped by adding acetic acid when Tau was phosphorylated to 0.4–0.5 phosphates per Tau molecule. Dephosphorylation of CDK5-Tau peptides was performed with 5 units of alkaline phosphatase at 37°C for 4 hr. The IMAC procedure in this study followed the vender instructions. Phos-Select iron affinity gel (100 μl) was incubated with Tau phospho-peptides. The binding condition of Tau peptides and IMAC resin was 250 mM acetic acid in 25% acetonitrile. Bound peptides were eluted in 150 mM ammonuion hydroxide in 25% acetonitrile. In microtubule-associated protein experiments, 250 μg of heat-stable proteins were treated with sequencing-grade trypsin at a ratio of 50:1 (proteins: trypsin) in 50 mM ammonium bicarbonate at 37°C for 16 hr. All peptides (synthetic and expressed) were transferred to PlusOne Mini dialysis bags with 1 kDa cut-off (Amersham Bioscience) and dialyzed against water at 4°C overnight. A C18 reverse phase chromatography may be used to substitute the dialysis step. Lyophilized peptides were stored at –20°C for the subsequent capture-release-tag procedure and mass spectrometry.

Mass Spectrometry

MALDI-TOF mass spectrometric analysis of synthetic peptides was performed in a Voyager DE-STR MALDI-TOF mass spectrometer (Applied Biosystems, Foster City, CA) in the positive ion, delayed-extraction, and reflector-on mode. General settings of the MALDI-TOF experiments were as follows: accelerating voltage 20,000 V, grid voltage 75%, guide wire 0.02%, extraction delay time 200 ns. Peptide samples were desalted with ZipTip C18 preloaded tips (Millipore, Bedford, MA). Bound peptides were eluted from the tips with 2 μl of a solution containing 10 mg/ml α-cyano-4-hydroxycinnamic acid, 50% acetonitril, 10% ethanol, and 0.1% TFA solution and spotted directly onto a gold-coated target plate. For the analysis of microtubule-associated proteins, a Micro Q-TOF system was used (Waters, Milford, MA). The system includes a HPLC liquid chromatography (CapLC) online-coupled with a nano-electrospray

ionization quadrupole-time of flight instrument. Cleaved products derived from a starting material of 500 μg peptide samples (Tau, CDK5-Tau, and PKA-Tau) or 250 μg heat-stable samples were injected into the HPLC system equipped with a PicoFrit C18 column (New Objective, Woburn, MA). Mixtures of peptides were resolved in a 90 min gradient (5%–40% of acetonitrile) with a flow rate of 0.8 μl/min. The top three strongest ion peaks in parent-ion-scan mode (m/z 400–2000, 1 s/scan) were automatically selected for subsequent CID analysis (m/z 90–2000, 1.5 s/scan). Collision energy in CID analysis used a default mass-charge-dependent profile provided by the vender. TFA-cleaved tagged peptides, which were derived from a starting material of 10 μg peptides, were also analyzed with the same system. Mixtures of peptides were resolved in a 120 min gradient (5%–40% of acetonitrile) with a flow rate of 0.8 μl/min. Collision energy in CID used a default mass-charge-dependent profile provided by the vender. The ion-trap tandem mass spectrometry was carried out at NanoApplication Scientific (Medford, MA). The mass spectrometer LCQ Deca XP was coupled to a micro-spray Vydac C18 column HPLC system and operated by Xcalibur 1.2 XP1 software.

Analysis of Mass Spectrometric Data

Raw data obtained from Q-TOF tandem mass spectrometric analysis was processed with MassLynx 4.0 software (Waters, Milford, MA) to generate peak lists. Raw data acquired from ion-trap tandem mass spectrometric analysis was processed with Biowork 3.1 software (Thermo Electron, CA) to generate peak lists. Peak lists of each sample were submitted to a Mascot server (Matrixscience, London, UK) and searched against the SwissProt protein database. Unmatched peak lists were further submitted to the Mascot server against a customized MAP-Tau database. Tolerance of parent ions and daughter ions were 1.5 and 0.6 Daltons, respectively. Minimal Mascot score was set to 26 for the first data filtration. All Mascot results were also crossexamined with their corresponding CID spectra manually to ensure fidelity of the computational outcome.

Supplemental Data

Supplemental Data include two figures and two tables and can be found with this article online at http://www.chembiol.com/cgi/content/full/12/7/769/DC1/.

Acknowledgments

H.-C.T. is supported by a Howard Hughes Medical Institute fellowship. H.O. is supported by the Netherlands Foundation for Scientific Research (NWO). L.-H.T. is an Investigator of the Howard Hughes Medical Institute. We thank Andrea Musacchio at European Institute of Oncology, Italy, for providing crystallography-grade CDK5/p25 complex. This work is supported by the Howard Hughes Medical Institute and a pilot grant from Harvard Center of Neurodegeneration and Repair Core C. We thank Benedikt Kesseler and Hermen Overkleeft for helpful discussion and Christopher Frank and Laura L. Yerkes for critical reading of the manuscript. This research was conducted under no financial interest from any contributing author.

Received: March 3, 2005
Revised: April 28, 2005
Accepted: May 3, 2005
Published: July 22, 2005

References

1. Pandey, A., and Mann, M. (2000). Proteomics to study genes and genomes. Nature *405*, 837–846.
2. Edelman, A.M., Blumenthal, D.K., and Krebs, E.G. (1987). Protein serine/threonine kinases. Annu. Rev. Biochem. *56*, 567–613.
3. Hunter, T. (1995). Protein kinases and phosphatases: The yin and yang of protein phosphorylation and signaling. Cell *80*, 225–236.
4. Mann, M., Ong, S.E., Gronborg, M., Steen, H., Jensen, O.N., and Pandey, A. (2002). Analysis of protein phosphorylation using mass spectrometry: Deciphering the phosphoproteome. Trends Biotechnol. *20*, 261–268.
5. Meyer, H.E., Hoffmann-Posorske, E., and Heilmeyer, L.M., Jr. (1991). Determination and location of phosphoserine in proteins and peptides by conversion to S-ethylcysteine. Methods Enzymol. *201*, 169–185.
6. Oda, Y., Nagasu, T., and Chait, B.T. (2001). Enrichment analysis of phosphorylated proteins as a tool for probing the phosphoproteome. Nat. Biotechnol. *19*, 379–382.
7. Knight, Z.A., Schilling, B., Row, R.H., Kenski, D.M., Gibson, B.W., and Shokat, K.M. (2003). Phosphospecific proteolysis for mapping sites of protein phosphorylation. Nat. Biotechnol. *21*, 1047–1054.
8. McLachlin, D.T., and Chait, B.T. (2003). Improved beta-elimination-based affinity purification strategy for enrichment of phosphopeptides. Anal. Chem. *75*, 6826–6836.
9. Qian, W.J., Goshe, M.B., Camp, D.G., 2nd, Yu, L.R., Tang, K., and Smith, R.D. (2003). Phosphoprotein isotope-coded solid-phase tag approach for enrichment and quantitative analysis of phosphopeptides from complex mixtures. Anal. Chem. *75*, 5441–5450.
10. Annan, W.D., Manson, W., and Nimmo, J.A. (1982). The identification of phosphoseryl residues during the determination amino acid sequence in phosphoproteins. Anal. Biochem. *121*, 62–68.
11. Brittain, S.M., Ficarro, S.B., Brock, A., and Peters, E.C. (2005). Enrichment and analysis of peptide subsets using fluorous affinity tags and mass spectrometry. Nat. Biotechnol. *23*, 463–468.
12. Goedert, M., Spillantini, M.G., Jakes, R., Rutherford, D., and Crowther, R.A. (1989). Multiple isoforms of human microtubule-associated protein tau: Sequences and localization in neurofibrillary tangles of Alzheimer's disease. Neuron *3*, 519–526.
13. Tseng, H.C., Lu, Q., Henderson, E., and Graves, D.J. (1999). Phosphorylated tau can promote tubulin assembly. Proc. Natl. Acad. Sci. USA *96*, 9503–9508.
14. Grundke-Iqbal, I., Iqbal, K., Tung, Y.C., Quinlan, M., Wisniewski, H.M., and Binder, L.I. (1986). Abnormal phosphorylation of the microtubule-associated protein tau (tau) in Alzheimer cytoskeletal pathology. Proc. Natl. Acad. Sci. USA *83*, 4913–4917.
15. Grundke-Iqbal, I., Iqbal, K., Quinlan, M., Tung, Y.C., Zaidi, M.S., and Wisniewski, H.M. (1986). Microtubule-associated protein tau. A component of Alzheimer paired helical filaments. J. Biol. Chem. *261*, 6084–6089.
16. Hanger, D.P., Betts, J.C., Loviny, T.L., Blackstock, W.P., and Anderton, B.H. (1998). New phosphorylation sites identified in hyperphosphorylated tau (paired helical filament-tau) from Alzheimer's disease brain using nanoelectrospray mass spectrometry. J. Neurochem. *71*, 2465–2476.
17. Reynolds, C.H., Betts, J.C., Blackstock, W.P., Nebreda, A.R., and Anderton, B.H. (2000). Phosphorylation sites on tau identified by nanoelectrospray mass spectrometry: differences in vitro between the mitogen-activated protein kinases ERK2, c-Jun N-terminal kinase and P38, and glycogen synthase kinase-3β. J. Neurochem. *74*, 1587–1595.
18. Liu, F., Iqbal, K., Grundke-Iqbal, I., and Gong, C.X. (2002). Involvement of aberrant glycosylation in phosphorylation of tau by cdk5 and GSK-3β. FEBS Lett. *530*, 209–214.
19. Dhavan, R., and Tsai, L.H. (2001). A decade of CDK5. Nat. Rev. Mol. Cell Biol. *2*, 749–759.
20. Tseng, H.C., Zhou, Y., Shen, Y., and Tsai, L.H. (2002). A survey of Cdk5 activator p35 and p25 levels in Alzheimer's disease brains. FEBS Lett. *523*, 58–62.
21. Patrick, G.N., Zukerberg, L., Nikolic, M., de la Monte, S., Dikkes, P., and Tsai, L.H. (1999). Conversion of p35 to p25 deregulates Cdk5 activity and promotes neurodegeneration. Nature *402*, 615–622.
22. Lin, J.H., and Chiang, B.H. (1996). A modified procedure for caseinophosphopeptide analysis. J. Chromatogr. Sci. *34*, 358–361.
23. Maux, D., Enjalbal, C., Martinez, J., and Aubagnac, J.L. (2002). New example of proline-induced fragmentation in electrospray ionization mass spectrometry of peptides. Rapid Commun. Mass Spectrom. *16*, 1470–1475.

24. Michel, G., Mercken, M., Murayama, M., Noguchi, K., Ishiguro, K., Imahori, K., and Takashima, A. (1998). Characterization of tau phosphorylation in glycogen synthase kinase-3beta and cyclin dependent kinase-5 activator (p23) transfected cells. Biochim. Biophys. Acta *1380*, 177–182.
25. Ishiguro, K., Omori, A., Sato, K., Tomizawa, K., Imahori, K., and Uchida, T. (1991). A serine/threonine proline kinase activity is included in the tau protein kinase fraction forming a paired helical filament epitope. Neurosci. Lett. *128*, 195–198.
26. Paudel, H.K., Lew, J., Ali, Z., and Wang, J.H. (1993). Brain proline-directed protein kinase phosphorylates tau on sites that are abnormally phosphorylated in tau associated with Alzheimer's paired helical filaments. J. Biol. Chem. *268*, 23512–23518.
27. Baumann, K., Mandelkow, E.M., Biernat, J., Piwnica-Worms, H., and Mandelkow, E. (1993). Abnormal Alzheimer-like phosphorylation of tau-protein by cyclin-dependent kinases cdk2 and cdk5. FEBS Lett. *336*, 417–424.
28. Illenberger, S., Zheng-Fischhofer, Q., Preuss, U., Stamer, K., Baumann, K., Trinczek, B., Biernat, J., Godemann, R., Mandelkow, E.M., and Mandelkow, E. (1998). The endogenous and cell cycle-dependent phosphorylation of tau protein in living cells: implications for Alzheimer's disease. Mol. Biol. Cell *9*, 1495–1512.
29. Lund, E.T., McKenna, R., Evans, D.B., Sharma, S.K., and Mathews, W.R. (2001). Characterization of the in vitro phosphorylation of human tau by tau protein kinase II (cdk5/p20) using mass spectrometry. J. Neurochem. *76*, 1221–1232.
30. Cruz, J.C., Tseng, H.-C., Goldman, J.A., Shih, H., and Tsai, L.-H. (2003). Aberrant Cdk5 activation by p25 triggers pathological events leading to neurodegeneration and neurofibrillary tangles. Neuron *40*, 471–483.
31. Goedert, M., Crowther, R.A., and Garner, C.C. (1991). Molecular characterization of microtubule-associated proteins tau and MAP2. Trends Neurosci. *14*, 193–199.
32. Sanchez, C., Diaz-Nido, J., and Avila, J. (2000). Phosphorylation of microtubule-associated protein 2 (MAP2) and its relevance for the regulation of the neuronal cytoskeleton function. Prog. Neurobiol. *61*, 133–168.
33. Tsuyama, S., Terayama, Y., and Matsuyama, S. (1987). Numerous phosphates of microtubule-associated protein 2 in living rat brain. J. Biol. Chem. *262*, 10886–10892.
34. Sanchez, C., Arellano, J.I., Rodriguez-Sanchez, P., Avila, J., DeFelipe, J., and Diez-Guerra, F.J. (2001). Microtubule-associated protein 2 phosphorylation is decreased in the human epileptic temporal lobe cortex. Neuroscience *107*, 25–33.
35. Songyang, Z., Blechner, S., Hoagland, N., Hoekstra, M.F., Piwnica-Worms, H., and Cantley, L.C. (1994). Use of an oriented peptide library to determine the optimal substrates of protein kinases. Curr. Biol. *4*, 973–982.
36. Lee, G., Newman, S.T., Gard, D.L., Band, H., and Panchamoorthy, G. (1998). Tau interacts with src-family non-receptor tyrosine kinases. J. Cell Sci. *111*, 3167–3177.
37. Lim, R.W., and Halpain, S. (2000). Regulated association of microtubule-associated protein 2 (MAP2) with Src and Grb2: Evidence for MAP2 as a scaffolding protein. J. Biol. Chem. *275*, 20578–20587.
38. Klein, C., Kramer, E.M., Cardine, A.M., Schraven, B., Brandt, R., and Trotter, J. (2002). Process outgrowth of oligodendrocytes is promoted by interaction of fyn kinase with the cytoskeletal protein tau. J. Neurosci. *22*, 698–707.
39. Liou, Y.C., Sun, A., Ryo, A., Zhou, X.Z., Yu, Z.X., Huang, H.K., Uchida, T., Bronson, R., Bing, G., Li, X., et al. (2003). Role of the prolyl isomerase Pin1 in protecting against age-dependent neurodegeneration. Nature *424*, 556–561.
40. Ficarro, S.B., McCleland, M.L., Stukenberg, P.T., Burke, D.J., Ross, M.M., Shabanowitz, J., Hunt, D.F., and White, F.M. (2002). Phosphoproteome analysis by mass spectrometry and its application to Saccharomyces cerevisiae. Nat. Biotechnol. *20*, 301–305.
41. Byford, M.F. (1991). Rapid and selective modification of phosphoserine residues catalysed by Ba2+ ions for their detection during peptide microsequencing. Biochem. J. *280*, 261–265.
42. Collins, M.O., Yu, L., Coba, M.P., Husi, H., Campuzano, I., Blackstock, W.P., Choudhary, J.S., and Grant, S.G. (2004). Proteomic analysis of in vivo phosphorylated synaptic proteins. J. Biol. Chem. *280*, 5972–5982.
43. Beausoleil, S.A., Jedrychowski, M., Schwartz, D., Elias, J.E., Villen, J., Li, J., Cohn, M.A., Cantley, L.C., and Gygi, S.P. (2004). Large-scale characterization of HeLa cell nuclear phosphoproteins. Proc. Natl. Acad. Sci. USA *101*, 12130–12135.
44. Kaiser, E., Colescott, R.L., Bossinger, C.D., and Cook, P.I. (1970). Color test for detection of free terminal amino groups in the solid-phase synthesis of peptides. Anal. Biochem. *34*, 595–598.